

Shape Discrimination with Hexapole–Dipole Interactions in Magic Angle Spinning Colloidal Magnetic Resonance

Pietro Tierno,^{*,†} Steffen Schreiber,[‡] Walter Zimmermann,[‡] and Thomas M. Fischer[‡]

*Departament de Química Física, Universitat de Barcelona, Martí i Franquès 1, 08028 Barcelona, Spain, and
Physikalisches Institut, Universität Bayreuth, 95440 Bayreuth, Germany*

Received November 12, 2008; E-mail: ptierno@ub.edu

Ⓜ This paper contains enhanced objects available on the Internet at <http://pubs.acs.org/jacs>.

Magic angle spinning (MAS) is a powerful technique in solid-state NMR that allows time averaging of the magnetic dipolar interactions between the nucleons, which in turn increases the spectral resolution.¹ Dipolar interactions and chemical shifts are both first-order anisotropies that are proportional to the second-order Legendre polynomial $P_2(\cos \vartheta)$ and therefore vanish when the sample is spun at the “magic angle” (ϑ_{magic}) of 54.7° with respect to the direction of the applied magnetic field. However, second-order anisotropies, such as quadrupolar and hexapole–dipole interactions, do not vanish at ϑ_{magic} , since they are proportional to the fourth-order Legendre polynomial [$P_4(\cos \vartheta_{\text{magic}}) = -7/18 \neq 0$], and thus can cause small but finite spectral broadening. Effects due to higher-order multipole moments play an important role in many other systems, such as in rare-earth compounds,² antiferroelectric liquid crystals,³ nematic molecules,⁴ electrorheological fluids,⁵ and nematic emulsions.⁶ It has been shown that liquid dispersions of paramagnetic colloidal particles can be used as a model system in condensed matter.^{7,8} When the system is subjected to an external magnetic field, the dipolar interactions between the particles can be precisely tuned. However, these particles have spherical shapes and thus cannot cause magnetic anisotropy and large multipolar interactions. In this work, we used dipole–dipole and dipole–hexapole interactions for shape-sensitive active control, assembly, and sorting of microscopic colloidal particles.

We studied the interactions between magnetically driven, DNA-linked anisotropic and isotropic colloidal rotors interacting via induced magnetic dipolar and multipolar forces. Anisotropic colloidal doublets were realized by using two streptavidin-coated polystyrene paramagnetic spherical particles having different radii, $a_1 = 1.4 \mu\text{m}$ and $a_2 = 0.5 \mu\text{m}$ (Dynabeads). The two particles were linked with two complementary single-stranded DNA sequences having 25 base pairs.⁹ A water drop containing $\sim 10^6$ doublets/mL was placed on top of a glass plate (see Figure 1a). Gravity and electrostatic interactions between the doublets and the negatively charged glass surface confine the particles to float a few nanometers above the surface. An external magnetic field was provided by using three coils with their axes perpendicular to each other. In comparison to MAS, where spinning is achieved by mechanically rotating a tilted sample, our magnetic field precesses with frequency Ω and precession angle ϑ about an axis normal to the glass plate supporting the rotors. The coil normal to the substrate was connected to a DC current source (TTi EX1810R), while the two horizontal coils were connected to a waveform generator (TTi TGA1242) fed by a current amplifier (ONKYO M-282). The particles were observed with a $100\times$ oil immersion objective mounted on an optical microscope (Leica DMPL) equipped with a CCD color camera (Basler A311F). Videos for image analysis were recorded at a rate of

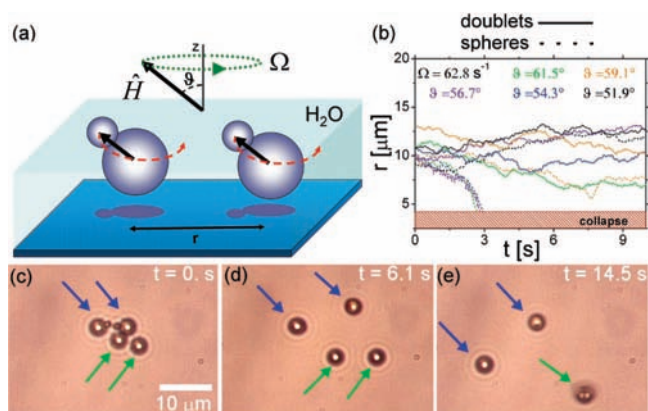


Figure 1. (a) Scheme of two doublets rotated by an external magnetic field \mathbf{H} precessing around the z axis with frequency Ω and precession angle ϑ . (b) Time evolution of the interparticle distances r for two interacting doublets (continuous lines) and two isotropic spheres (dashed lines) at various precession angles ϑ for $\Omega = 62.8 \text{ s}^{-1}$ and $H = 1300 \text{ A/m}$. (c–e) Images of the colloidal doublets (blue arrows) and isotropic spheres (green arrows). The precession angle was originally set to $\vartheta = 0$, causing all of the rotors to separate [(c) \rightarrow (d)]. We then switched the precession angle to $\vartheta = 56.7^\circ$, and the doublets remained separated while the spheres collapsed [(d) \rightarrow (e)]. The doublet shape visible in (c) can only be resolved when the particles are at rest.

Ⓜ A movie showing this behavior is available.

30 frames/s. At low frequencies ($\Omega < 75.4 \text{ s}^{-1}$), the colloidal rotors resonate and synchronously rotate with the field.

Mainly odd magnetic multipole moments¹⁰ m_l ($l = 1, 2, 3, \dots$) [e.g., $m_1 = (\chi_1 V_1 + \chi_2 V_2)H$ and $m_3 = 3(a_1 + a_2)^2 \chi_1 V_1 \chi_2 V_2 H / (\chi_1 V_1 + \chi_2 V_2)$, where V_1 and V_2 are the volumes of the individual spheres composing the doublet, $\chi_1 = 0.4$ and $\chi_2 = 1.1$ are the effective volume magnetic susceptibilities of the spheres, and $\hat{\mathbf{H}} = H\{(\cos \vartheta)\mathbf{e}_z + (\sin \vartheta)[\cos(\Omega t)\mathbf{e}_x + \sin(\Omega t)\mathbf{e}_y]\}$ is the precessing magnetic field] are induced in each rotor, and the rotors start to magnetically interact with each other. Higher moments occur only in rotors with anisotropic shapes, and this allows us to discriminate between isotropically and anisotropically shaped rotors close to ϑ_{magic} .

In the Supporting Information we provide a detailed description of the dynamics of an individual doublet with respect to the frequency of the applied magnetic field. Since here we are interested in the interactions between two rotors, all the measurements described below were made at low frequency, where the doublets rotate synchronously with the magnetic field. Using video microscopy and particle-tracking routines, we analyzed the time evolution of the relative displacement between the rotors. The solid lines in Figure 1b show the interparticle distance between two doublets as a function of time at different precession angles for $\Omega = 62.8 \text{ s}^{-1}$. Similar data for a pair of isotropic spheres under the same field conditions are shown as dashed lines. In the red-shaded region in Figure 1b, the rotors merge to form a single

[†] Universitat de Barcelona.

[‡] Universität Bayreuth.

rotating cluster. Changing the precession angle of the field allows the dipolar interaction between the rotors to be varied from net attractive (where all the particles collapse into a single rotating cluster) to net repulsive (where isotropic spheres and anisotropic doublets diffuse close to each other but do not collapse). Isotropic rotors are repulsive for $\vartheta < \vartheta_{\text{magic}}$ and attractive for $\vartheta > \vartheta_{\text{magic}}$. Thus, the isotropic rotors are well-described by dipolar coupling. The anisotropic doublets, however, are repulsive even for $\vartheta > \vartheta_{\text{magic}}$ (e.g., for ϑ up to 61.5° at $\Omega = 62.8 \text{ s}^{-1}$). In the discriminating range of precession angles $\vartheta_{\text{magic}} < \vartheta < 61.5^\circ$, isotropic particles can be extracted from a mixture of shapes because they all collapse into one rotating supercluster (Figure 1c–e). We attribute the stronger repelling tendency of anisotropic rotors to repulsive hexapole–dipole interactions.¹¹ We explored the range of precession angles for discriminating particles with different shapes by first applying a magnetic field precessing at an angle $\vartheta < \vartheta_{\text{magic}}$, where the four rotors separated as in Figure 1c,d. We then switched to a precession angle of $\vartheta = 56.7^\circ$, where the isotropic particles collapsed while the rotating doublets repelled and remained separated. A movie showing the separation dynamics of the four rotors, including the collapse of the spheres but not the doublets after switching to $\vartheta = 56.7^\circ$, is available. Two other movie files showing similar behavior are also available.⁹

We can explain the interaction between the rotating doublets by considering both the dipole–dipole ($F_{\text{dd}} \propto r^{-4}$) and dipole–hexapole ($F_{\text{dh}} \propto r^{-6}$) contributions to the total magnetic force F_{mag} :

$$F_{\text{mag}} = \frac{\mu_0}{4\pi} \left[3 \frac{m_1^2 P_2(\cos \vartheta)}{r^4} - 15 \frac{m_1 m_3 P_4(\cos \vartheta)}{r^6} \right] \quad (1)$$

where m_1 and m_3 are the dipole and hexapole moments of the doublet. If we neglect hydrodynamic interactions between the two rotors,⁹ the magnetic force on each rotor is balanced by the viscous drag $F_{\text{visc}} \approx 6\pi\eta a v/2$ on that rotor, where $a \approx a_1 + a_2 \cos^2(\vartheta/2)$ is the hydrodynamic radius of the spinning rotor, $\eta = 10^{-3} \text{ Ns/m}^2$ is the viscosity of water, and v is the relative velocity between the two rotors. Such an approximation holds for larger separations, and we obtain the attraction or repulsion velocity of the rotors as:

$$v = \frac{\mu_0 m_1^2}{4\pi^2 \eta a^5} \left[\frac{P_2(\cos \vartheta)}{(r/a)^4} - 5 \frac{m_3}{m_1 a^2} \frac{P_4(\cos \vartheta)}{(r/a)^6} \right] \quad (2)$$

In the regime $\vartheta_{\text{magic}} < \vartheta < 61.5^\circ$, two anisotropic rotors will separate until they reach an equilibrium distance r_{eq} :

$$r_{\text{eq}} = \sqrt{\frac{5m_3 P_4(\cos \vartheta)}{m_1 P_2(\cos \vartheta)}} \quad (3)$$

From the equilibrium separation of the doublets, $r_{\text{eq}} = 11.3 \mu\text{m}$, we determined a hexapole-to-dipole ratio of $m_3/m_1 = 3.4 \mu\text{m}^2$ at a precession angle of $\vartheta = 56.7^\circ$. When we increased the precession angle to $\vartheta > 61.5^\circ$, the equilibrium radius became smaller than the hydrodynamic radius, and the doublets collapsed into a single rotating cluster. Figure 2 shows the experimental collapse velocity (open circles) for two doublets subjected to an external magnetic field precessing with frequency $\Omega = 50.2 \text{ s}^{-1}$ at an angle $\vartheta = 66.3^\circ (> \vartheta_{\text{magic}})$. The solid line is a fit to eq 2 with a dipole moment of $m_1 = 3.4 \times 10^{-14} \text{ A m}^2$ and a hexapole moment of $m_3 = 1.35 \times 10^{-25} \text{ A m}^4$, corresponding to an m_3/m_1 ratio of $3.9 \mu\text{m}^2$. As shown in the inset, the dipole–dipole attraction F_{dd} overcomes the dipole–hexapole repulsion F_{dh} , leading to a net attraction. A theoretical estimate of the m_3/m_1 ratio gives a value of $1.1 \mu\text{m}^2$, which is close to the experimental value. The remaining factor of 2 could arise either from depolarization effects due to the polymer matrix of the colloidal particles or to an

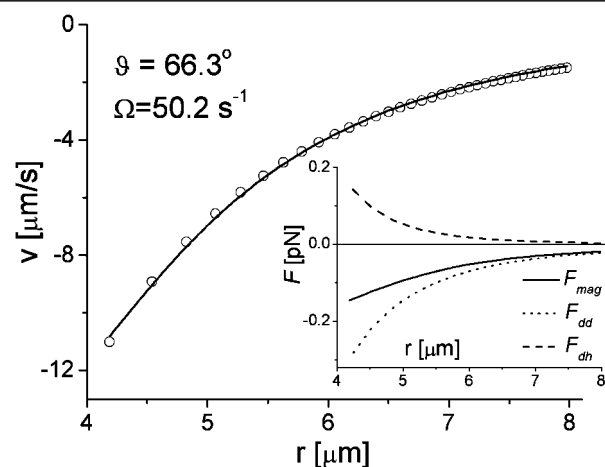


Figure 2. (a) Collapse velocity of two doublets under an external field with $\vartheta = 66.3^\circ$ and $\Omega = 50.2 \text{ s}^{-1}$. The solid line is a fit to eq 2. The inset shows the corresponding dipole (dotted line) and dipole–hexapole (dashed line) contributions to the total magnetic force (solid line) between the doublets.

asymmetric distribution of the superparamagnetic iron oxide grains inside the colloids.

In summary, we have realized micron-sized magnetically driven isotropic and anisotropic colloidal rotors. We have shown that a balance between magnetic dipole–dipole and dipole–hexapole interactions near the magic angle allows spherical and anisotropic magnetic colloidal rotors to be separated. The shape separation of externally controlled rotating micro-objects might be interesting for technological applications such as assemblies of stirrers for microfluidic devices,¹² microtechnological tools,¹³ and “reconfigurable” mechanical systems.¹⁴

Acknowledgment. The manuscript has benefited from stimulating discussions with Holger Stark. P.T. was supported in part by the program “Beatriu de Pinós” BP-B100167. T.M.F., S.S., and W.Z. acknowledge support from the German Science Foundation (DFG) via the research unit FOR608, and S.S. and W.Z. also acknowledge funding via the priority program SPP 1164.

Supporting Information Available: Realization of colloidal doublets, doublet rotation under a magnetic field, derivation of eq 1, discussion of the hydrodynamic interactions between the doublets, and two movies (AVI) showing the motions of doublets and spherical particles under a precessing magnetic field. This material is available free of charge via the Internet at <http://pubs.acs.org>.

References

- (1) Abragam, A. *Principles of Nuclear Magnetism*; Oxford University Press: Oxford, U.K., 1961.
- (2) Levy, P. M.; Morin, P.; Schmitt, D. *Phys. Rev. Lett.* **1979**, *42*, 1417.
- (3) Song, J.-K.; Fukuda, A.; Vij, J. K. *Phys. Rev. E* **2007**, *76*, 011708.
- (4) Pontü, S.; Freire, F. C. M.; Dias, J. C.; Evangelista, L. R. *Phys. Lett. A* **2008**, *372*, 43.
- (5) Chen, Y.; Sprecher, A. F.; Conrad, H. *J. Appl. Phys.* **1991**, *70*, 1.
- (6) Lubensky, T. C.; Petey, D.; Currier, N.; Stark, H. *Phys. Rev. E* **1998**, *57*, 610.
- (7) Mangold, K.; Leiderer, P.; Bechinger, C. *Phys. Rev. Lett.* **2003**, *90*, 158302.
- (8) Zahn, K.; Méndez-Alcaraz, J. M.; Maret, G. *Phys. Rev. Lett.* **1997**, *79*, 175.
- (9) See the Supporting Information.
- (10) For axisymmetric rotors, the magnetic multipole susceptibilities are scalar numbers defined with respect to the figure axis of the rotor.
- (11) Dipole–quadrupole interactions vanish because the precession axis is normal to the rotor separation.
- (12) Bleil, S.; Marr, D.; Bechinger, C. *Appl. Phys. Lett.* **2006**, *88*, 263515.
- (13) Galajda, P.; Ormos, P. *Appl. Phys. Lett.* **2001**, *80*, 4653.
- (14) Campbell, C. J.; Grzybowski, B. A. *Philos. Trans. R. Soc. London, Ser. A* **2004**, *362*, 1.

JA808888G